

Dynamics in an emergent quantum-like state space generated by a nonlinear classical network

Gregory D. Scholes

*Department of Chemistry, Princeton University, Princeton, NJ 08544, USA**

(Dated: April 1, 2025)

Abstract

This work exploits a framework whereby a graph (in the mathematical sense) serves to connect a classical system to a state space that we call ‘quantum-like’ (QL). The QL states comprise arbitrary superpositions of states in a tensor product basis. The graph plays a special dual role by directing design of the classical system and defining the state space. We study a specific example of a large, dynamical classical system—a system of coupled phase oscillators—that maps, via a graph, to the QL state space. We investigate how mixedness of the state diminishes or increases as the underlying classical system synchronizes or de-synchronizes respectively. This shows the interplay between the nonlinear dynamics of the variables of the classical system and the QL state space. We prove that maps from one time point to another in the state space are linear maps. In the limit of a strongly phase-locked classical network—that is, where couplings between phase oscillators are very large—the state space evolves according to unitary dynamics, whereas in the cases of weaker synchronization, the classical variables act as a hidden environment that promotes decoherence of superpositions.

* gscholes@princeton.edu

I. INTRODUCTION

In recent work we have described how a classical system can be mapped, via a graph representation, to a state space that has many properties similar to a quantum state space[1, 2]. For that reason, we call it a quantum-like (QL) state space, and refer to the states as QL states. The graphs needed as a basis for these constructions are called QL bits. Particular maps combine these special graphs to produce states that, remarkably, have the properties of quantum states. In particular, by applying a product operation to QL bit graphs we can produce graphs whose states comprise arbitrary (controllable) superpositions of states in a tensor product basis. These same graphs can also be used to define classical networks. In the present paper we study how dynamics of the classical networks are reflected in the properties of the QL states.

We study explicit examples where graphs map to classical states that are networks of coupled phase oscillators, therefore we can use the well-developed theories for synchronization phenomena to provide dynamical models for the classical network. The QL graph construction allows us to add a layer to the dynamical network—an associated state space in the tensor product basis. This is where the new results of this work lie. We explore the way synchronization and de-synchronization of the classical system encodes dynamics in the state space that can be described as purity-preserving dynamics and decoherence, respectively.

The QL bit graphs can represent physical, classical systems, most obviously networks of phase oscillators, as studied here. The crucial feature of QL bit graphs and the corresponding classical networks is that they encode two states. In our model, each state can be the emergent state of a subgraph of the QL bit graph, or we can choose the superpositions of emergent states as a basis. QL states, more generally, are represented by product graphs. Generally, these product graphs can be considered to be abstract systems, but they can also be produced by physical systems, such as networks. Here we make no assumptions about the physical manifestation of the phase oscillator system underlying the QL bits, but we could imagine it to represent some kind of dynamical structure of fields or particles that collectively form a microscopic QL object[3–5]. Or, more abstractly, these underlying variables might be thought of as an intuitive way of

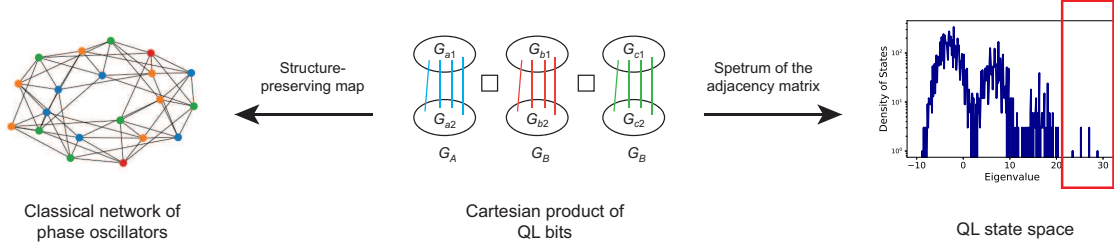


FIG. 1. Depiction of how the QL state graphs serve to direct, on one hand, the construction of a representative classical system, and on the other hand, a corresponding QL state space.

representing wavelike properties of a quantum particle because they capture the nature of phase. On the other hand, it can simply be a macroscopic classical network, for which there are numerous examples[6, 7]. Regardless of these possible interpretations, here we study the specific case of coupled phase oscillators serving as a classical system defined by a QL state graph, and a corresponding state space generated by the adjacency matrix of that graph.

In Fig. 1 the correspondence between the classical system of phase oscillators and the graph and the QL state space is shown. The graph plays a special dual role by directing design of the classical system and defining the state space. The QL state space, specifically, comprises the set of states, projected out of the eigenvectors of the adjacency matrix, that are indicated by the emergent states, highlighted by the box over the spectrum. The interplay between the classical system and these states comes about in the the present work by the evolution of the oscillator phases. We say more about how we configure the classical system in relation to the state space in the next section of the paper.

We develop the idea that there are two viewpoints for our system. First, we can observe the nonlinear dynamics of the complex classical network either at a very detailed classical level, or by considering a global order parameter. Second, we can study the state space in the reduced representation of the emergent QL states. The graph model for QL states[1] connects these two viewpoints. What seems particularly interesting about the parallel view of the *same* dynamics, is that it offers a way to think about the underlying classical variables that control properties of the QL state space—those variables can be hidden if we imagine we can only observe the state space and do

not know much, or anything, about the classical system that is controlling the states. However, they are not necessarily deterministic, depending how we define the averaging (see the next section).

II. HOW GRAPHS MAP CLASSICAL VARIABLES TO THE STATE SPACE

To start, we briefly provide some background. A graph $G(n, m)$, or simply G , comprises n vertices and a set of m edges that connect pairs of vertices. The size of a graph or subgraph, that is, the number of vertices, is written $|G|$. A graph has two important features. First, the structure of the graph—determined by the pattern of edges—plays a key role in the classical dynamical evolution of a system represented by the graph. That is because the structure of couplings between phase oscillators in the network plays an important role in determining phase synchronization[8–11]. Second, any graph can be characterized by its spectrum and associated eigenstates. Each (finite) graph is represented by a matrix called the adjacency matrix, A , and the spectrum of a graph is obtained by diagonalizing the corresponding adjacency matrix. The adjacency matrix is indexed by the vertices and (for a normal graph) contains an entry 1 at a_{ij} if the vertex i is linked by an edge to vertex j . We can assign a phase (or bias) to the edges so that they may take any value on the unit circle in the complex plane[12–14]. We will exploit this freedom in the present work to map a classical network of phase oscillators to a graph. Here we will specialize to undirected graphs, so the adjacency matrix is symmetric ($a_{ij} = a_{ji}$). For more specialized background on graph theory see [15–17].

Special graphs, called expander graphs, have a spectrum comprising a distinguished emergent state—a state that is clearly separated from other states in the spectrum. The emergent state of an expander graph is the resource we use to construct the QL state space. Two expander graphs are bound by connecting edges to produce a two-state system that we call the QL bit[1]. These QL bit graphs are combined using a graph operation—the Cartesian product of graphs—to generate a new, exponentially larger, graph. The states of this product graph are linear combinations of tensor products of the states of the QL bits[2]. For background see ref [18].

Hidden variable theories in quantum mechanics aim to enable a physical interpretation of quantum mechanics, in particular to address questions such as how measurement works, what is the relationship between quantum and classical theories, and so on[19–32]. The main scope of hidden variable theories is to ask whether there is a deterministic system with predetermined outcomes prescribed for its properties, but this picture is hidden to us by the ways we measure the state vector. The motivation is that the hidden picture would clarify some of the mysteries that underpin the quantum theory. The no-hidden-variables theorems show how this is not the case[20].

Another program is to understand how superpositions might collapse under dynamics governed by a modified version of the Schrödinger equation[3, 33–35]. Here the challenge is to understand how superpositions are lost, which is impossible under the linear evolution of the Schrödinger equation. Solving that problem would explain why macroscopic systems are not found in superposition and the theory would thus demystify the quantum to classical transition. One proposal is that the Schrödinger equation is modified so that at the micro-scale it appears unchanged from our usual formulation, but at longer length scales a nonlinear, stochastic feature emerges[34]. This new feature acts to collapse superpositions. In this program, details of the nonlinear feature are hidden when we measure the state vectors.

In the present work, we study a different way of imagining a hidden nonlinear system. By connecting a classical system to a state space (here the QL state space), we can explore how concrete properties of the classical system affect the states. We consider networks of phase oscillators for the classical system, so the implications of phase in the state vectors comes to the forefront. We can ask, for example, whether collapse of superposition is possible in an isolated system because of the way the states are generated by a system that cannot lock the phases of the states? To explore this question we set up a map from a complex classical system to a quantum-like state space that is mediated by properties of a suitable graph. An appropriate state space is provided by the graph representation for a QL bit[1], combined with the Cartesian product operation on the graphs to produce a new graph that generates a state space mimicking arbitrary quantum states[2]. The classical system we consider here, as mentioned, is a network of phase oscillators. The structure of that network is templated by the graphs

that generate the QL state space.

Any QL state space is mirrored by a corresponding graph. That graph can be considered to be an abstract concept, but can also be physically realized. A notable example is the system of phase oscillators studied here. Each oscillator is specified by a vertex in the graph and the edges show which phase oscillators are pairwise coupled. Notice here that the classical system is related one-to-one with the graph structure, although this is not a general requirement of the mapping of the classical system to the state space via a graph. The graph, or equivalently the network of phase oscillators, is much more complex than the state space because we reduce the state space to include only the emergent states (Sec. IV.B). The many other ‘random’ states in the spectrum[18] are ignored. Thus, the complexity of the graph, or classical system, is reduced in the QL state space.

The evolution of the oscillator system, though sensitive to the specified initial conditions, is entirely deterministic. However, we use a particular averaging over the initial conditions that reflects our hypothesis that we cannot know the initial phases of the oscillators, only the variance of the distribution. Therefore, in the numerical studies we take an ‘ensemble’ average over initial conditions of the phase oscillators which is intended to capture the fact that we cannot know precisely the phases. It is not necessarily an average over a set of distinct QL systems. Details of the classical system are therefore obscured in the state space by the unknown phases of the oscillators.

In this report, we study how dynamics of the classical system compares to, and governs, dynamics in the QL state space. The basis for the study are the nonlinear dynamics of a large, complex classical network of phase oscillators. We ask, how are these dynamics reflected in the reduced space of QL states?

III. SYNCHRONIZATION

The literature on synchronization phenomena is vast[6, 36–42]. The idea of collective motion is well known to us from everyday experiences, and provides a good concrete example of physical synchronization[43, 44]. There are numerous examples in biology, from circadian rhythms to cell cycles to neural networks to ensembles of atoms[45–51].

To explain the mechanism underlying synchronization, we review the Van der Pol method, using a derivation reproduced from Chapter 12 of ref [7]. Consider the quasi-linear oscillator equation,

$$\ddot{x} + \omega_0^2 x = \mu f(x, \dot{x}) \quad (1)$$

where the dots indicate differentiation with respect to time. We re-write the equation in the equivalent form

$$\dot{x} = y \quad (2)$$

$$\dot{y} = -\omega_0^2 x = \mu f(x, y) \quad (3)$$

where $0 < \mu \ll 1$ is a small parameter that determines how close the system is to a linear conservative system. Now define polar coordinates

$$\rho = \sqrt{x^2 + y^2 / \omega_0^2}$$

$$\tan \theta = \omega_0 x / y$$

then find that Eqs 2, 3, with $\mu = 0$ reduce to the phase paths of the harmonic oscillator, that is, circles about the origin:

$$x = \rho \cos(\omega_0 t + \theta) \quad (4)$$

$$y = -\rho \omega_0 \sin(\omega_0 t + \theta) \quad (5)$$

For $\mu \neq 0$, we apply the identity $\cos(A+B) = \cos A \cos B - \sin A \sin B$ and the product rule to obtain from Eqs 2–5

$$\dot{\rho} \cos(\phi) - \rho \sin(\phi) \dot{\theta} = 0 \quad (6)$$

$$-\dot{\rho} \omega_0 \sin(\phi) - \rho \omega_0 \cos(\phi) \dot{\theta} = \mu f(x, y) \quad (7)$$

where $\phi = \omega_0 t + \theta$, $x = \rho \cos \phi$, and $y = -\rho \omega_0 \sin \phi$. The solutions are written

$$\dot{\rho} = \frac{-\mu f(x, y) \sin \phi}{\omega_0} \quad (8)$$

$$\dot{\phi} = \omega_0 - \frac{\mu f(x, y) \cos \phi}{\rho \omega_0} \quad (9)$$

Typically ρ is slowly varying compared to ϕ . The nonlinearity can arise for various reasons, and is reflected in $f(x, y)$, case by case. For example, the pendulum clock is

subjected to regular, short pushes that counteract dissipative losses of the pendulum. Electronic oscillator circuits incorporate a nonlinear element that, with the right conditions, enables the circuit to produce sustained oscillations because of feedback between the oscillatory system and the nonlinear element.

In the case of a system of many interacting oscillators, the Kuramoto model[36, 39] attributes the nonlinearity to the coupling among the oscillators:

$$\dot{\theta}_i = \nu_i - \frac{K}{N} \sum_{j=1}^N a_{ij} \sin(\theta_j - \theta_i), \quad (10)$$

where ν_i is the frequency of the oscillator at node i , θ_i is the oscillator phase defined in terms of accumulated phase and an offset $\theta_i(t) = \epsilon_i t + \phi_i$. K is the coupling value, a_{ij} (with value 0 or 1) are taken from the adjacency matrix of the graph representing the node connectivities in the network, and the coupling is renormalized by the factor $1/N$ so that networks are size-intensive with respect to the lowest eigenvalue.

This remarkably simple system of equations predicts how oscillators collectively synchronize, according to the chosen parameters such as frequency disorder, coupling strength, and initial phases of the oscillators. Feedback introduced by small coupling between pairs of oscillators causes oscillators to speed up or slow down during a period of oscillation—according to their natural frequency relative to the mean—ultimately equilibrating to a steady state where, for some initial conditions, phases remain locked in step. It is entropically favorable to minimize $\theta_{ij} = \theta_j - \theta_i$ because otherwise the system has to maintain a sequence of correlations among the evolving phases, decided by the sum rule for angles in an n -gon, $\sum \theta_{ij} = \pi(n - 2)$. That influences the allowed phase differences. For example, consider three oscillators in the network (i, j, k) , where we know θ_{ij} and θ_{ik} , then we must have that $\theta_{kj} = \pi - \theta_{ij} - \theta_{ik}$. Thus many correlations are embedded in the coupling matrix.

The propensity for a system of oscillators to synchronize depends on the form of the coupling matrix, that is, the structure of the graph where each oscillator is represented by a vertex and pairwise coupling is indicated by an edge[8, 52]. Synchronization also tends to be more robust when many oscillators are coupled, provided that the couplings are global. Notably, systems with only nearest-neighbor coupling synchronize poorly compared to more highly connected networks[9, 52].

Collective synchronization in an oscillator ensemble comprising N oscillators is quantified by the order parameter, where $\text{Re}(x)$ means the real part of x :

$$\text{order parameter} = \text{Re}\left(\frac{1}{N} \sum_{i=1}^N e^{i\theta_i}\right). \quad (11)$$

A connection between this synchronization model and random matrix theory was established in ref [53]. In that work we considered a network of phase oscillators defined by a graph and considered a Gaussian distribution of frequencies for the oscillators. It was noted that an ensemble of synchronization trajectories, each started with a random phase distribution for the oscillators, equilibrated to a phase distribution representative of the order parameter and indicative of the standard deviation of the frequency distribution. That is, for example, when the standard deviation of the frequency distribution is less than the coupling K , but not much less, then the equilibrium phases are clustered with a certain circular standard deviation, which can be related to the frequency distribution. It was thus proposed that the equilibrium properties of the phase oscillator ensemble can be predicted using a phase-oscillator version of random matrix theory. A relevant finding is that the states of a poorly synchronized phase oscillator network are more mixed than those of a synchronized network. We use a related method in the calculations of spectra and states described below.

IV. PHASE OSCILLATOR SYNCHRONIZATION AND DYNAMICS IN THE STATE SPACE

A. Phase and the adjacency matrix

Here we examine the relationship between, on the one hand, dynamics of a nonlinear classical system, and on the other hand, the evolution of the state space interpreted by the graph representation. The model we use here is to assign each vertex of the graph as a phase oscillator, and the edges indicate couplings between pairs of phase oscillators. Thus we can use the Kuramoto model to explore the synchronization dynamics of the classical network of phase oscillators. The oscillators (vertices) are connected according to the graph model for QL bits and their products. This provides a physical realization of the classical variables associated with the QL states. We concomitantly calculate

the states and their dynamics as the network synchronization evolves. It will turn out that this gives insight into, and a tangible physical model for, the implications of phase relationships between the variables underlying QL states.

The eigenvectors we have described in prior work are calculated for the normal adjacency matrices of the graphs (i.e. edges have values ± 1). They correspond to the states of perfectly globally-synchronized systems. More generally, however, each oscillator labeled j is associated with a phase θ_j . The adjacency matrix A is transformed by these phases according to:

$$A' = \Phi^{-1} A \Phi, \quad (12)$$

with

$$\Phi = \begin{bmatrix} e^{i\theta_1} & 0 & 0 & \dots \\ 0 & e^{i\theta_2} & 0 & \dots \\ 0 & 0 & \ddots & 0 \\ 0 & \dots & 0 & e^{i\theta_{2n}} \end{bmatrix} \quad (13)$$

This unitary transformation of A does not change the spectrum, but it does rotate the basis for the eigenstates. We use this transformation below, after defining projection of the emergent states, to show how the eigenvectors of the projected emergent states transform under continuous rotations. Later in this paper, we use the transformation of Eq. 13 to account for how oscillator phases in the classical network dictate the eigenvector basis. That basis change, in general, varies throughout the ensemble and therefore influences the mixedness of the state[53]. Recall that we use the term ‘ensemble’ to mean an average over initial phases.

Notice that the matrix Φ lists the phase of each oscillator in the system, associating each phase to a vertex representing an oscillator. Recall that this phase is the sum of accumulated phase associated with the frequency offset from the mean and a phase offset, $\theta_i(t) = \epsilon_i t + \phi_i$. The transformation weights edges in the graph by phase *differences*. Thus, for an edge connecting vertex j to vertex k , the entry in the upper triangular part of the adjacency matrix transforms as $1 \rightarrow \exp(-i[\theta_j - \theta_k])$, with the corresponding complex conjugate map in the lower triangular part. The diagonal elements remain as entries of 0.

In the numerical examples shown below we obtain the phases from simulations using

the Kuramoto model, described in the previous section. For any time point during the simulation, we use the oscillator phases to define Φ , then we diagonalize $\Phi^{-1}A\Phi$ to obtain the eigenvectors of the emergent states—now with complex coefficients. We project these coefficients to those for an effective two-state system for each QL bit, as we now describe for the example of a single QL bit. The method is generalized in the obvious way for a system comprising any number of QL bits.

B. The effective 2-state model for QL bit emergent states

Our basis for the states of the QL bit is defined by the vertices of the graph, G_A , which we enumerate in terms of each subgraph as basis states $\{u_1, u_2, \dots, u_n\}$ for subgraph G_{a1} , and $\{x_1, x_2, \dots, x_k\}$ for subgraph G_{a2} , given $|G_{a1}| = n$ and $|G_{a2}| = k$. Taken together, we have a complete orthonormal basis in $\mathbb{C}^{(n+k)}$.

An arbitrary emergent state, W , of the QL bit graph will be written in terms of this basis as:

$$W = c_1 u_1 + \dots + c_n u_n + d_1 x_1 + \dots + d_k x_k \quad (14)$$

where the c_i and d_j are complex coefficients. Now define

$$J_{a1} = \underbrace{\{1, 1, \dots, 1\}}_{n \text{ times}} \underbrace{\{0, 0, \dots, 0\}}_{k \text{ times}} / \sqrt{n} \quad (15)$$

$$J_{a2} = \underbrace{\{0, 0, \dots, 0\}}_{n \text{ times}} \underbrace{\{1, 1, \dots, 1\}}_{k \text{ times}} / \sqrt{k}. \quad (16)$$

We resolve the coefficients for the effective two-states of the QL bit in terms of the basis associated to the subgraphs G_{a1} and G_{a2} , $|a_1\rangle$ and $|a_2\rangle$ using the inner products

$$\alpha = \langle J_{a1}, W \rangle \quad (17)$$

$$\beta = \langle J_{a2}, W \rangle \quad (18)$$

to give

$$W_{2 \times 2} = \alpha |a_1\rangle + \beta |a_2\rangle. \quad (19)$$

Some examples of coefficients for the effective two-states of a QL bit are provided in Fig. 2. Each panel shows a vector representation of the complex coefficients of $W_{2 \times 2}$

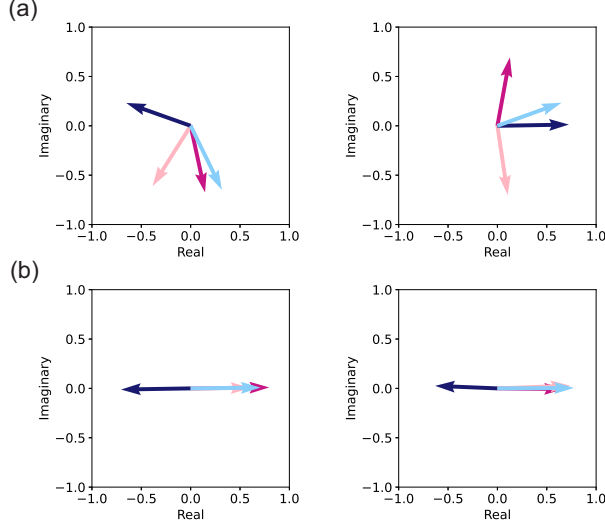


FIG. 2. Vector representation of the complex coefficients of $W_{2 \times 2}$ corresponding to the highest eigenvalue (α_0 is violet red, β_0 is light pink) and the second highest eigenvalue (α_1 is dark blue, β_1 is light blue). (a) Examples of systems comprising partially synchronized oscillators. (b) Examples of systems where the oscillators are synchronized.

corresponding to the highest eigenvalue (α_0 is violet red, β_0 is light pink) and the second highest eigenvalue (α_1 is dark blue, β_1 is light blue). Fig. 2a shows the eigenvectors for partially synchronized oscillators in one QL bit, derived from phases early in the dynamics of a phase oscillator system with initially random phases. The simulation used the same parameters as detailed later for the simulations of synchronization on the product graph of two QL bits. These coefficients contrast to those obtained for the synchronized oscillators in one QL bit, where phases were obtained later in the simulation once the oscillators has synchronized, Fig. 2b.

C. Phase in the states

For a synchronized oscillator system on the QL bit graph with all edges set to 1 in the adjacency matrix, we find that $\alpha_0 = \beta_0 \approx 1/\sqrt{2}$ and $\alpha_1 = -\beta_1 \approx 1/\sqrt{2}$ (we use the convention that β_1 takes the negative sign). More generally, we can bias the edges that connect the two subgraphs by giving them values (in the adjacency matrix) of any value on the unit circle in the complex plane. Recall that the special case of negative-signed

edges connecting the subgraphs can be interpreted as phases of the two subgraphs being perfectly out of phase[1]. The resulting eigenvectors can be evaluated by considering the effective adjacency matrix for the QL bit graph comprising two d -regular subgraphs coupled by edges given the bias $e^{i\alpha}$:

$$A_{2 \times 2} = \begin{bmatrix} d & e^{i\alpha} \\ e^{-i\alpha} & d \end{bmatrix}, \quad (20)$$

which gives an eigenvector for the emergent state $(e^{i\alpha}, 1)$ and for the state associated with the next eigenvalue $(-e^{i\alpha}, 1)$. These states are obtained by continuous rotation of the connecting edge bias. Note that we have neglected an overall phase of these states. When that phase is accounted for, then we see that the emergent state is any vector in \mathbb{C}^2 . By rotating the edge bias, we therefore generate states (when the system is perfectly synchronized) that emulate, for example, the states of a system of spins or polarization states of photons. The notable emergent states isomorphic to polarization states of light are: (i) the linear combinations $a_1 \pm a_2$, when edges take values ± 1 respectively, which are comparable to linear combinations of vertical and horizontal polarization; (ii) the states $a_1 \pm ia_2$, when edges take values of $\pm i$, analogous to right- and left-circularly polarized light.

D. Synchronization of quantum bits

An explicit theory for synchronization of quantum bits was proposed by Lohe[54–56]. The theory is developed by writing a generalized non-Abelian version of the Kuramoto model for coupled n -level systems:

$$i\hbar \dot{U}_i U_i^\dagger = H_i - \frac{iK}{2N} \sum_{j=1}^N a_{ij} (U_j U_i^\dagger - U_i U_j^\dagger). \quad (21)$$

Here, H_i is a constant $n \times n$ Hermitian matrix with eigenvalues being the natural frequencies of each oscillator (that is, the mean frequency plus the offset from the mean). The U_i are $n \times n$ complex unitary matrices. Setting $n = 1$ gives $U_i = e^{-i\theta_i}$, recovering the Kuramoto model. Setting

$$U_i = \begin{bmatrix} \alpha_i & -\beta_i \\ \bar{\beta}_i & \bar{\alpha}_i \end{bmatrix} = \begin{bmatrix} w_i + iz_i & y_i + ix_i \\ -y_i + ix_i & w_i - iz_i \end{bmatrix} \quad (22)$$

yields a theory for predicting synchronization dynamics of N coupled two-level quantum systems (quantum bits). The matrix in Eq. 22 can be written as a real unit 4-vector $\mathbf{x}_i = (x_i, y_i, z_i, w_i)$, defining how each qubit vector lies on \mathbb{S}^3 . The vectors evolve under the continuous group operations of $\text{SU}(2)$. Unsynchronized quantum bits are seen as the U_i dispersed around \mathbb{S}^3 , whereas synchronized quantum bits lock into phase on the manifold.

The Lohe model can be considered to be a specialized version of the model we study here because, first, it locks the phases of vertices within each QL bit and, second, it applies to the single excitation subspace of the tensor product basis. In the Kuramoto model, we can imagine synchronization of phase oscillators to require a choreographed speeding up of low-frequency oscillators and slowing of high-frequency oscillators. This happens because of the way the interaction between all pairs of oscillators depends explicitly on their phase difference, via $\sin(\theta_j - \theta_i)$. Owing to the way we have set up the graphs to represent two-state systems—QL bits—we can apply the Kuramoto model to the oscillators and effectively synchronize QL bits. That is, our graph construction of QL bits can simply be used with the Kuramoto model. Whereas if we choose to treat vertices as qubits, then we should apply the Lohe model. These two approaches become similar (in principle yielding identical predictions) when phases are strongly synchronized within each QL bit graph, but arbitrary between graphs. The phase difference enters in a more complicated way in the Lohe model for coupled quantum bits, as we now outline.

Lohe[55] writes the H_i so as to indicate the way each oscillator traces out a periodic path on \mathbb{S}^3 (under the continuous group operations of $\text{SU}(2)$):

$$H_i = \sum_j \omega_i^j \sigma_j = \begin{bmatrix} \omega_i^3 & \omega_i^1 - i\omega_i^2 \\ \omega_i^1 + i\omega_i^2 & -\omega_i^3 \end{bmatrix} \quad (23)$$

where ω_i^j are the frequencies of the vector in \mathbb{S}^3 , ω_i^1 , ω_i^2 , and ω_i^3 . For intuition about what the three frequencies mean, recall that a vector moving on \mathbb{S}^2 , the unit sphere embedded in 3-dimensional space, can be indicated by the frequencies it sweeps out

over two angles, the azimuthal angle and the polar angle. Then, for the unit 3-sphere, in 4-dimensional space, we need three unique angles.

Now, substituting Eqs. 22 and 23 into Eq. 21, Lohe obtained

$$\dot{\mathbf{x}}_i = \Omega_i \mathbf{x}_i - \frac{K}{N} \sum_{j=1}^N a_{ij} [\mathbf{x}_j - \mathbf{x}_i (\mathbf{x}_j \cdot \mathbf{x}_i)] \quad (24)$$

where

$$\Omega_i = \omega_i \cdot \mathbf{L} = \omega_i^1 L_1 + \omega_i^2 L_2 + \omega_i^3 L_3,$$

with the \mathbf{L} being the 4×4 skew symmetric matrices[57]:

$$L_1 = \begin{bmatrix} 0 & 0 & 0 & -1 \\ 0 & 0 & -1 & 0 \\ 0 & 1 & 0 & 0 \\ 1 & 0 & 0 & 0 \end{bmatrix},$$

$$L_2 = \begin{bmatrix} 0 & 0 & 1 & 0 \\ 0 & 0 & 0 & -1 \\ -1 & 0 & 0 & 0 \\ 0 & 1 & 0 & 0 \end{bmatrix},$$

$$L_3 = \begin{bmatrix} 0 & -1 & 0 & 0 \\ 1 & 0 & 0 & 0 \\ 0 & 0 & 0 & -1 \\ 0 & 0 & 1 & 0 \end{bmatrix}.$$

From Eq. 24 we can see that synchronization now is promoted by the nonlinearity induced by the pairwise relationships between unit 4-vectors $\mathbf{x}_j - \mathbf{x}_i (\mathbf{x}_j \cdot \mathbf{x}_i)$.

It seems that we can emulate this synchronization of quantum bits by building a system of QL bits, interacting via edges connecting vertices of one QL bit to another. For consistency with the Lohe model, we would require each QL bit to comprise strongly synchronized oscillators, and to be synchronized. The emergent state of each QL bit gives its frequency. We can assign a random initial ‘phase’ as the real 4-vector vector in \mathbb{S}^3 that defines the orientation of the eigenvector of the synchronized emergent state. The key point is that this vector, associated to $|\psi_i\rangle$ in Eq. 6 of Ref. [55], must represent the emergent state vector as an element that sweeps through values in \mathbb{C}^2 , and we have established this to be the case.

The system of N QL bits would be combined into a new graph $G = G_A \oplus G_B \oplus \dots \oplus G_N$. The subgraphs are connected by edges, weighted so that the inter-QL bit coupling is weaker than the coupling between vertices within a QL bit. The graphs G_A, G_B, \dots are the vertices of the Lohe model. This system of oscillators, propagated according to the Kuramoto model, will mimic the Lohe model. To compare the results we should project out the effective 2-state emergent states of each QL bit to construct the vectors \mathbf{x}_i .

We do not report these numerical calculations here, but provide the strategy for the following reasons. First, we will refer to this model in a later section of the paper. Second, by proposing how a model comprising a system of coupled classical phase oscillators can predict the same results as a system of coupled quantum bits emphasizes how the QL model succeeds in various ways to produce state spaces very much like those enjoyed by quantum systems.

V. SYNCHRONIZATION VERSUS DECOHERENCE OF QL STATES

A. Methods

Here we study a network phase oscillator model with a coupling structure templated by the Cartesian product of two QL bit graphs $G_A \square G_B$. The phase oscillators are indicated by vertices of the graph, and are assigned a phase that biases the edges, as we describe below.

In the numerical simulations, each graph comprises n_0 vertices, giving a total of $N = n_0 \times n_0$ vertices in the product graph. Each subgraph $G_{a1}, G_{a2}, G_{b1}, G_{b2}$ comprises 20 vertices (therefore $n_0 = 40$) and is d -regular with $d = 15$. Edges between subgraphs were added randomly, with probability 0.2. We calculate the full Cartesian product, yielding $2d$ -regular subgraphs in $G_A \square G_B$, with an eigenvalue of 30 for the emergent state when the subgraphs are uncoupled (that is, neglecting eigenvalue shift labeled Δ in Ref. [2]). We expect four emergent states, two with an eigenvalue of 30, one at $30 + \Delta$, and one at $30 - \Delta$.

The graph provides the coupling map for a system of N phase oscillators that we model using the Kuramoto model, Eq. 10. Couplings between vertices are weighted

uniformly by K/N , with K chosen to be 250 for the first set of calculations. Vertices are assigned a mean frequency of 100 in the same arbitrary units as K , and offset by frequencies randomly selected from a normal distribution with standard deviation 1 and mean of 0 (in the same arbitrary units). Initial phases for the oscillators are randomly assigned from a von Mises distribution with circular standard deviation of either 50, meaning the distribution is similar to a uniform distribution, or 0.001, meaning the distribution is extremely narrow. Results are averaged over either 100 or 500 realizations of this set-up. See ref [53] for some background and examples that might be helpful. The coupling $K/N = 0.5625$ is moderately strong compared to the ratio of the standard deviation of the frequency distribution to its mean, 0.01.

The main motivation for the ensemble averaging over realizations of the system is to account for uncertainty in the initial oscillator phases. Therefore, we use the term ‘ensemble’ to mean an average over initial conditions of oscillator phase. The initial phase for any oscillator means its natural frequency and its phase offset, ϵ_i and ϕ_i , respectively. This setup for the calculations means that the dynamics are not strictly deterministic, because we do not know the initial conditions precisely. We also report calculations where we, additionally, average over an ensemble of graphs. In fact, because the subgraphs are d -regular (with no edges randomly deleted like we showed in prior work[1]), the ensemble comprises graphs with different configurations of edges connecting the subgraphs.

During the evolution of the system, the phase of each oscillator θ_i evolves nonlinearly, as discussed in the previous section. At selected time points we transform the adjacency matrix of the graph according to Eqs. 12, 13, which introduces phase differences by weighting the edges between vertices j and k by $e^{i(\theta_k - \theta_j)}$. We average the spectrum of the transformed adjacency matrix over all iterations of the simulation to give ensemble spectra. The spectra were computed for various time points, and therefore order parameters, as the system synchronized.

Before discussing these results, we note that although the phases of the initial distribution of oscillators are randomly distributed, the phase differences contain embedded correlations—there are N phases, but much more than N phase differences. However, the phase differences are uncorrelated from one simulation to another, so mixedness

comes from an essential ensemble averaging over simulations. In prior work mixedness as a function of synchronization was studied in some detail[53].

In Eq. 12 we are applying a unitary transformation to the adjacency matrix. Therefore the spectrum does not change with order parameter, only the state. The density matrix for the relevant emergent state is calculated in the basis produced by the effective two-state model for each QL bit. That is, we statistically average over the pure states:

$$\Psi(t) = c_1(t)|a_1\rangle|b_1\rangle + c_2(t)|a_2\rangle|b_1\rangle + c_3(t)|a_1\rangle|b_2\rangle + c_4(t)|a_2\rangle|b_2\rangle, \quad (25)$$

for each time point in a simulation. Here the $c_i(t)$ are complex coefficients obtained from the projections outlined in Sec. IV.B, and the basis states are the emergent states from each subgraph. For example, for subgraph G_{a1} the emergent state is $|a_1\rangle$ and for subgraph G_{a2} the emergent state is $|a_2\rangle$. From the ensemble of $\Psi(t)$ we determine the density matrix $\rho(t)$ in the product basis, with entries

$$\rho_{ij}(t) = \langle c_i(t)c_j^*(t) \rangle \quad (26)$$

where the angle brackets mean an average over the ensemble of simulations. We report $\text{Tr}(\rho)^2$ as a simple measure of mixedness of the state.

B. Synchronization

We now describe numerical results for a network of phase oscillators that are connected in a way prescribed by the product of two QL bits. For these calculations, we have performed an average over initial phases as well as an average over 500 graphs (see Methods). First, we set the initial phase distribution to be, essentially, the uniform distribution and the coupling to be relatively strong, $K = 250$. These conditions allow us to observe synchronization of the oscillators. The line in Fig. 3a shows the ensemble average order parameter, Eq.11, predicted by propagating Eqs. 10 over 80 periods of the mean natural frequency of the oscillators. At early time the order parameter is small because the initial condition specifies a near uniform phase distribution. As time increases, the order parameter increases to approximately 1, showing that the nonlinear evolution of the phase oscillator system synchronizes the oscillator phases.

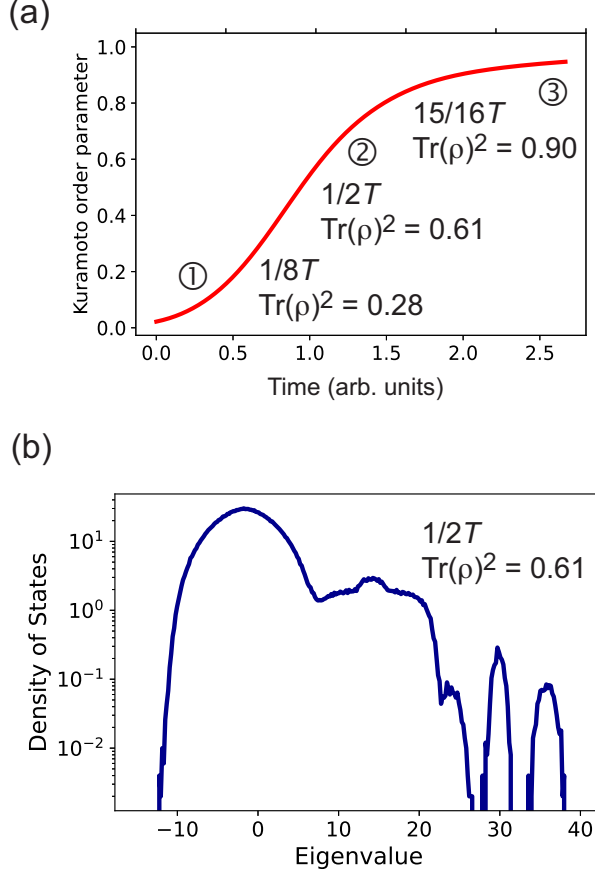


FIG. 3. (a) Ensemble-averaged Kuramoto order parameter as a function of time predicted for the system of oscillators. The time points corresponding to the plots of spectra are indicated together with the purity calculated at that time point. The time points are indicated as a fraction of the total time of the simulation. (b) Spectra calculated at one representative time point.

Concomitantly, the state associated with the greatest eigenvalue in the spectrum of the state space represented by the graph becomes less mixed. The state evolves in the effective state space by Eq. 26, according to the time dependence of the coefficients. We highlight this result for the time points labeled numerically in Fig. 3a. Corresponding spectra are all identical, as expected. An example is plotted in Fig. 3b. Purity of the state with greatest eigenvalue is indicated together with the time point, written as a fraction of the total time of the simulation. For example, $\frac{1}{8}T$ equates to 10 periods of oscillation. Note that the purity for a fully mixed system of dimension 4, with a

diagonal density matrix, is 0.25 (see Sec. 4d of Ref. [58]). The initial purity of 0.25 means that the state is mixed because we have no information about the phases of the oscillators. As the phases synchronize, the variance of the phases diminishes, and the purity increases. The relationship between phase distribution and purity is discussed in Ref. [53].

Despite the fact that the underlying synchronization dynamics are inherently non-linear, maps in the state space taking the state from one time point to another, $\Xi : \rho(t_1) \rightarrow \rho(t_2)$, are linear maps.

Proposition 1 *Maps of quantum-like (QL) states $\Xi : \rho(t_1) \rightarrow \rho(t_2)$ generated by a classical system of coupled phase oscillators are linear maps.*

To prove the proposition, first note that we construct each state ρ as a convex combination of ρ_j taken from trajectories indexed by j . Recall that the statistical averaging was done to account for an unknown initial phase distribution of the oscillators. So, given M trajectories in the ensemble,

$$\frac{1}{M} \sum_j \rho_j(t_1) \rightarrow \frac{1}{M} \sum_j \rho_j(t_2),$$

which is obviously linear. It remains to consider maps within each trajectory that take the pure state $\rho_j(t_1)$ to $\rho_j(t_2)$. This amounts to examining maps of the coefficients in Eq.25. Consider the map $X : \Phi_j(t_1) \rightarrow \Phi_j(t_2)$, where $\Phi_j(t_k)$ is the matrix of oscillator phases, Eq. 13, for trajectory j at time point t_k . X simply takes the phases for the oscillators at time point t_1 and transforms them to the new phases at t_2 , that is, changing each phase indexed by i by $\Delta\theta_i = \theta_i(t_2) - \theta_i(t_1)$. The map is the matrix containing $e^{i\Delta\theta_i}$ at each diagonal entry i . Thus, $\Phi_j(t_2) = X\Phi_j(t_1)$, where X is a linear map. Then, by using the facts that unitary maps are linear and compositions of linear maps are linear, the proposition is proved.

Moreover, the Ξ are trace-preserving completely positive maps[59–62] because they map $\rho \rightarrow \rho'$. However, the dynamical evolution is generally not unitary; being unitary only in the limit of strong synchronization.

Different regimes can be identified. When all the oscillators are strongly synchronized within each QL bit, but not necessarily between QL bits, then the general model for

the single-excitation subspace specializes to the Lohe model. Single-excitation subspace means that the network graph carries the structure of the tensor *sum* of QL bit graphs and QL bits are coupled to other QL bits. When the coupling K for the classical system is very weak compared to the standard deviation of the frequency distribution, then the oscillators cannot synchronize and the QL states remain mixed. When the coupling is very large, then the oscillator system is locked in phase. In this regime, dynamics in the QL state space can be unitary. That is, when the oscillators remain synchronized, the dynamics preserve purity.

We show this purity-preserving regime in Fig. 4. After an initial period when the oscillators synchronize, the system settles to equilibrium dynamics where the oscillators are locked in a limit cycle, that is, a closed, isolated (stable) phase trajectory. Owing to the way we define the oscillator network of each QL bit, these stable dynamics involve classical superpositions of oscillators local to each subgraph. In the corresponding state space, we find that when the classical system is synchronized, the purity of the emergent state is approximately 1. The observed dynamics in the state space are purity-preserving. In this regime, dynamics that ensue from abruptly changing basis, applying a driving field, imposing quantum quench conditions, and so on, can be unitary. To explore this regime in future work, it would be useful to define the properties of the QL state graphs a little differently. For example, we can assign a frequency ω_1 to vertices in the subgraph G_{a1} and $\omega_2 \neq \omega_1$ to vertices in the subgraph G_{a2} , thereby allowing the two states of the QL bit to have a frequency gap.

In the section, we have generalized our prior model, allowing any phase for the edges. We generalized the model further by explicitly considering the degree of phase synchronization in the classical network. The extent of synchronization of the underlying classical network controls the mixedness of the emergent states. Hence, this property of the variables defined by the classical network influences an important property of the states—phase coherence of the basis states is essential for sustaining stable superposition states. Depending on the properties of the of the classical phase oscillator network, the QL states can exhibit purity-preserving dynamics, or they can be completely mixed and undergo classical dynamics, or any case in between. When the oscillator network is synchronized, that is, the phases are coherent, then the QL states have high purity.

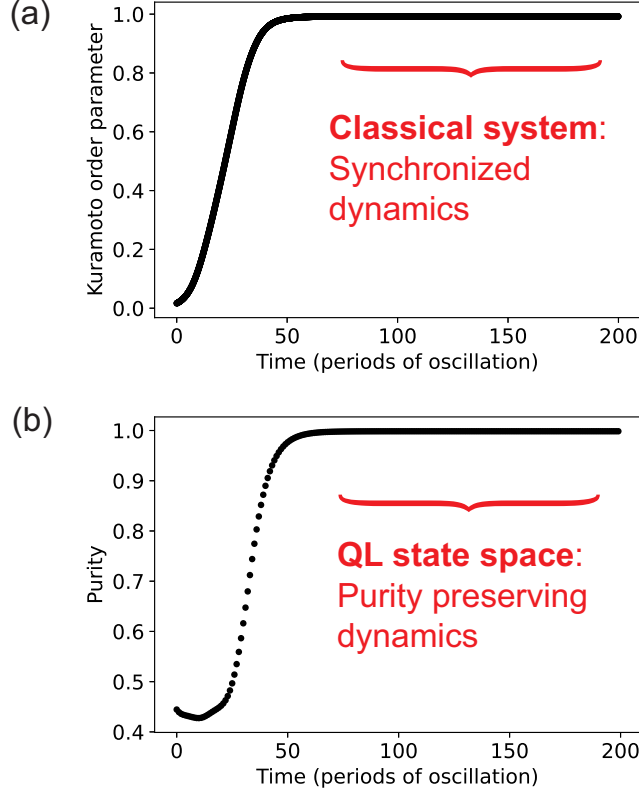


FIG. 4. (a) Ensemble-averaged Kuramoto order parameter as a function of time predicted for the system of oscillators. The system equilibrates to limit cycle dynamics, indicating a synchronized classical system. (b) The state space concomitantly evolves to an equilibrium of purity-preserving dynamics.

Physically, this phase coherence is similar to properties of a wave-like system underlying the states.

C. Decoherence

We have focused on synchronization of the classical network to produce robust QL states. Conversely, we hypothesize that a poorly synchronized network will decohere a pure QL state associated with an initially synchronized classical network. That is, the opposite dynamics to those illustrated in Fig. 4 will ensue. An obvious example is a network of uncoupled oscillators with a frequency distribution. Starting in-phase, free evolution of the oscillators will dephase the order parameter and states in the network.

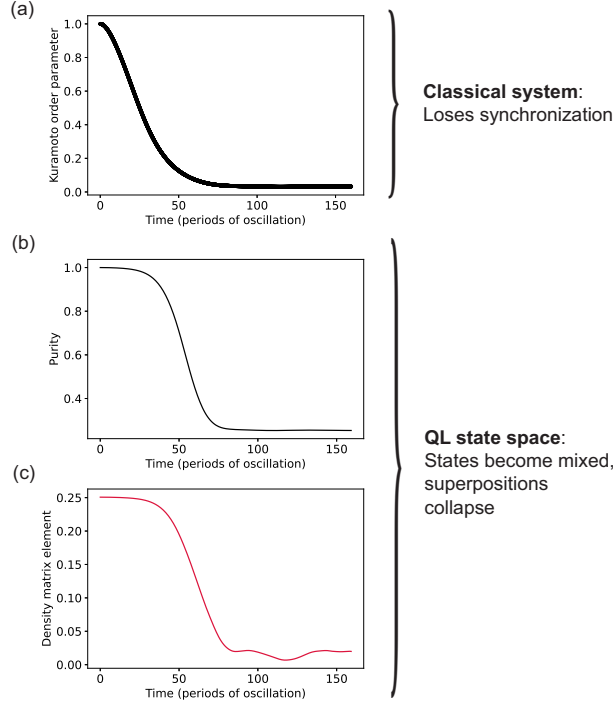


FIG. 5. Results of calculations of an oscillator system comprising the Cartesian product of two QL bits, using the same procedures and parameters as the previous calculations, except here we set the coupling to be weak, $K = 30$ and the initial condition sets all the oscillators in phase. Here the averaging is carried out over a single graph. (a) The order parameter, initially 1, indicating the initial synchronization condition, decays as the oscillators become out of phase. (b) As the oscillators dephase, the purity of the emergent state decays to an equilibrium mixed state. (c) Concomitantly, off-diagonal elements of the density matrix in the product basis decay to zero, highlighting loss of superpositions.

In Fig. 5 we show results of calculations of an oscillator system comprising the Cartesian product of two QL bits, using most of the same procedures and parameters as the previous calculations. Two key parameters were changed: the coupling was set to be weak, $K = 30$, and the initial condition sets all the oscillators in phase. We show results from two similar sets of calculations. One where we average only over the initial phase conditions. In the other calculation we average also over the ensemble of graphs.

In each case, the average is over 500 realizations of the system.

The order parameter is initially 1, indicating the initial synchronization condition, then it decays as the oscillators become out of phase. The dephasing is initiated by the fastest and slowest oscillators losing synchronization, which disconnects the network sufficiently so that, at a critical time in the evolution, all oscillators rapidly lose synchronization. This happens essentially by free evolution of the oscillators according to their natural frequencies because the coupling is too small to enforce synchronization. Accompanying the loss of synchronization, the purity of the mixed state decays. The fully mixed state has a purity of 0.25 because the density matrix is that for a four-state system[58].

The model captures the concept of an isolated QL system that succumbs to decoherence spontaneously. The numerical study shows an example of an initial pure state that decays to a final, equilibrium, state that is fully mixed in the product basis. The superpositions between basis states are completely lost, as evidenced by decay of the off-diagonal elements of the density matrix in the product basis, Fig. 5c. The classical variables—the phase oscillator network—control the coherence of the state, such that the quantum state space is slaved to the dynamics of the network. When the network is poorly synchronized, its many degrees of freedom act as a kind of environment that decoheres the states[63]. Imagine if we could only observe the state space, because the classical system was hidden somehow. Then we would observe spontaneous collapse of superpositions, Fig. 5b,c.

D. Discussion

We have studied the interplay between a classical system and a corresponding state space. A key point is that the classical system has the structure needed to encode the state space in a suitable product basis, in terms of states of each graph. This is achieved by constructing a classical network based on the Cartesian product of the constituent QL bit graphs. As a result of the product operation, the classical system necessarily acquires exponential complexity with the number of QL bits.

The underlying classical system not only provides a mechanism for producing the QL

state space, but, in addition, it actively controls the states. Owing to the complexity of the classical system (the system of coupled phase oscillators), it serves as a kind of bath, endowing the QL system with intrinsic properties like those characteristic of an open quantum system. For example, the system may exhibit *intrinsic* decoherence[64]. In this moderate coupling regime for the phase oscillator system, that is, the choice of coupling, K , relative to the distribution of natural frequencies of the oscillators, the state space undergoes dynamics that we call QL dynamics. The states are actively controlled by the dynamics of underlying system, which might be hidden from an observer. The example shown in Fig. 4 is that the mixedness of the emergent QL state decreases as the oscillators in the classical system synchronize. Whereas, in Fig. 5 we show a case where the mixedness of the emergent QL state *increases* as the oscillators in the classical system *de-synchronize*.

The model studied here suggests a way to understand a smooth QL to classical transition in the state space. This would be observed if the propensity of the classical network to synchronize diminishes as the size of the system increases. An open question, therefore, is whether (and how) there can be a distance dependence governing the decoherence so that distant superpositions naturally collapse. For example, we can imagine that the noise that gives the oscillators the frequency distribution is correlated on molecular length scales, but uncorrelated on longer length scales. This setup might serve to collapse distant superpositions, but preserve superpositions among closely-spaced systems.

Another possibility is that synchronization diminishes, after some cut-off, as more and more QL graphs are included in the product graph. A setup with this property (to consider in future work) is to endow the network and corresponding graph with a cut-off distance for couplings, or edges. In other words, the graph is d -regular, but only over a certain spatial extent and for the vertices that are included in that spatial area. The graph is everywhere d -regular, but two domains that are separated by a distance much greater than the cutoff are not fully connected. We can imagine this as a window that we can slide over the graph such that anywhere within the window the graph is d -regular. In this scenario, synchronization has a size limit. So, when the network enlarges as more QL bits are included in the product, there will be a point where the

entire state space cannot be coherent. The poorly connected network domain will limit the QL state space by acting as a bath and introducing decoherence. This kind of construction might give a small system—that is, smaller than the ‘window’—that is QL, but as the system is enlarged, the properties of its state space would become more classical (mixed). Here we have in mind that synchronizability of the classical network is a function of the number of vertices.

Thinking along these lines could enable a connection to be made to work aiming for a unified theory for the dynamics of microscopic and macroscopic systems, in particular, aiming to explain a mechanism for how superposition states can spontaneously collapse[3, 34, 35, 65]. Those studies incorporate a term into the Schrödinger equation that has no effect for typical quantum states, but for distant superpositions a stochastic, nonlinear term emerges that can initiate collapse of superpositions. The model considered in the present work appears to produce a similar result. We posited a somewhat different mechanism than proposed in prior important papers[3, 34, 35, 65] because in the present work the nonlinearity comes from the dynamics of the explicit classical system underlying the state space and it only controls phases of the underlying variables. The crucial parameter that impacts the states is the phase coherence of the classical network. However, the net result would be a modification of the Schrödinger equation prediction of dynamics in the state space. Indeed, we have noted how, when the oscillator network is poorly synchronized, it acts as a kind of bath for the state space. Thereby, it introduces a mechanism for decoherence similar to models for open quantum systems[66], where a system interacts with an external bath comprising many degrees of freedom. There is therefore an interesting connection between the models.

VI. CONCLUSIONS

We studied a specific example of a large classical system that maps, via a graph, to a state space that we call *quantum like* (QL) because it mimics the kinds of states typical of quantum systems. The classical system is a network of coupled phase oscillators, of the kind extensively studied in a wide variety of contexts. Such networks of coupled phase oscillator evolve according to the nonlinear dynamics associated with

synchronization of the oscillator phases. We reported numerical simulations for dynamics of this system, starting from an initial condition of a random distribution of oscillator phases. The network topology was blueprinted by a graph that generates the QL states. We used the phases of the classical system to weight the edges of the QL state graph at various time points during the dynamics, then mapped those graphs to the QL state space. Studying the state space, we constructed the density matrix in an effective basis of two coupled QL bits and showed that the mixedness of the emergent state diminished as the underlying classical system synchronized.

Similarly, decoherence of an initially synchronized system was exhibited by starting the dynamics of a weakly-coupled phase oscillator system with initial conditions where all the oscillators were in phase. During that simulation, the oscillators came out of phase, and the emergent state become concomitantly mixed. The superpositions of states in the product basis collapse, evidenced by the decay of off-diagonal elements in the density matrix. Increasing mixedness and spontaneous collapse of superpositions is caused by loss of synchronization among the many classical degrees of freedom (modeled as phase oscillators). We likened the many degrees of freedom of these variables to a kind of intrinsic ‘bath’. The QL state space therefore evolved, for the chosen parameters, like an open quantum system. Based on these results it is proposed that in the opposite limit, of a strongly phase-locked classical network—that is, where couplings between phase oscillators are very large so the classical system remains synchronized—the state space can evolve unitarily. We see evidence for this regime as the purity-preserving dynamics in the equilibrium emergent states of a synchronized network.

Key conclusions of the work are that nonlinear dynamics in the classical system controls the dynamics in the state space. The dynamics can help quantum-like states be robust to noise and disorder, or they can act like an intrinsic environment to produce decoherence in the state space. We showed numerical studies of both scenarios. Nevertheless, these dynamics convey linear maps in the state space (Prop. 1). This setup suggests a mechanism by which underlying variables act to collapse superpositions between product basis states in the QL system. The concept suggests a plausible mechanism that could potentially be generalized to explain the quantum-to-classical transition.

ACKNOWLEDGMENTS

This research was funded by the National Science Foundation under Grant No. 2211326 and the Gordon and Betty Moore Foundation through Grant GBMF7114. I thank Andrei Khrennikov for suggesting the idea of comparing dynamics of the network to dynamics in the state space.

- [1] G. D. Scholes, Quantum-like states on complex synchronized networks, *Proc. R. Soc. A* **480**, 20240209 (2024).
- [2] G. D. Scholes and G. Amati, Quantum-like product states constructed from classical networks, *Phys. Rev. Lett.* **134**, 060202 (2025).
- [3] A. Bassi, K. Lochan, S. Satin, T. P. Singh, and H. Ulbricht, Models of wave-function collapse, underlying theories, and experimental tests, *Rev. Mod. Phys.* **85**, 471 (2013).
- [4] P. D. Drummond and M. D. Reid, Retrocausal model of reality for quantum fields, *Phys. Rev. Res.* **2**, [10.1103/PhysRevResearch.2.033266](https://doi.org/10.1103/PhysRevResearch.2.033266) (2020).
- [5] E. B. Davies, Quantum stochastic processes, *Commun. Math. Phys.* **15**, 277 (1969).
- [6] S. Strogatz, *Sync: How order emerges from chaos in the Universe, Nature, and Daily Life* (Hyperion, New York, 2003).
- [7] V. Nekorkin, *Introduction to nonlinear oscillations* (Wiley-VCH, 2015).
- [8] P. Abdalla, A. S. Bandeira, M. Kassabov, V. Souza, S. H. Strogatz, and A. Townsend, Expander graphs are globally synchronizing, submitted **xx**, <https://doi.org/10.48550/arXiv.2210.12788> (2023).
- [9] M. Kassabov, S. H. Strogatz, and A. Townsend, A global synchronization theorem for oscillators on a random graph, *Chaos* **32**, 093119 (2022).
- [10] M. Kassabov, S. H. Strogatz, and A. Townsend, Sufficiently dense kuramoto networks are globally synchronizing, *Chaos* **31**, 073135 (2021).
- [11] A. Townsend, M. Stillman, and S. H. Strogatz, Dense networks that do not synchronize and sparse ones that do, *Chaos* **30**, 083142 (2020).
- [12] T. Zaslavsky, Biased graphs. i. bias, balance, and gains, *J. Comb. Theory Ser. B* **47**, 32

- (1989).
- [13] R. Mehatari, M. R. Kannan, and A. Samanta, On the adjacency matrix of a complex unit gain graph, *Lin. Multilin. Algebra* **70**, 1798 (2022).
 - [14] N. Reff, Spectral properties of complex unit gain graphs, *Lin. Alg. Appl.* **436**, 3165 (2012).
 - [15] R. Diestel, *Graph Theory* (Springer, Hamburg, 2017).
 - [16] S. Janson, T. Łuczak, and A. Ruciński, *Random Graphs* (Wiley Interscience, New York, 2000).
 - [17] B. Bollobás, *Random Graphs* (Cambridge University Press, Cambridge, 2001).
 - [18] G. D. Scholes, Graphs that predict exciton delocalization, *R. Soc. Phil. Trans. A* **xxx**, submitted (2024).
 - [19] S. Kochen and E. P. Specker, The problem of hidden variables in quantum mechanics, *J. Math. Mech.* **17**, 59 (1967).
 - [20] N. D. Mermin, Hidden variables and the two theorems of john bell, *Rev. Mod. Phys.* **803**, 803 (1993).
 - [21] M. Toros, S. Donadi, and A. Bassi, Bohmian mechanics, collapse models and the emergence of classicality, *J. Phys. A: Math. Theor.* **49**, 355302 (2016).
 - [22] D. Paneru, E. Cohen, R. Fickler, R. W. Boyd, and E. Karimi, Entanglement: quantum or classical?, *Rep. Prog. Phys.* **83**, [10.1088/1361-6633/ab85b9](#) (2020).
 - [23] O. Guehne, E. Haapasalo, T. Kraft, J.-P. Pellonpaa, and R. Uola, $\text{ij}\text{ colloquium:ij}$ incompatible measurements in quantum information science, *Rev. Mod. Phys.* **95**, [10.1103/RevModPhys.95.011003](#) (2023).
 - [24] M. Zurel, C. Okay, and R. Raussendorf, Hidden variable model for universal quantum computation with magic states on qubits, *Phys. Rev. Lett.* **125**, [10.1103/PhysRevLett.125.260404](#) (2020).
 - [25] S. S. Bhattacharya, S. Saha, T. Guha, and M. Banik, Nonlocality without entanglement: Quantum theory and beyond, *Phys. Rev. Res.* **2**, [10.1103/PhysRevResearch.2.012068](#) (2020).
 - [26] C. Budroni, A. Cabello, O. Guehne, M. Kleinmann, and J.-A. Larsson, Kochen-specker contextuality, *Rev. Mod. Phys.* **94**, [10.1103/RevModPhys.94.045007](#) (2022).

- [27] D. Bohm and J. Bub, A proposed solution of the measurement problem in quantum mechanics by a hidden variable theory, *Rev. Mod. Phys.* **38**, 453 (1966).
- [28] S. Peil, Proposed test of relative phase as a hidden variable in quantum mechanics, *Found. Phys.* **42**, 1523 (2012).
- [29] .
- [30] P. Grangier, Contextual inferences, nonlocality, and the incompleteness of quantum mechanics, *Entropy* **23**, [10.3390/e23121660](#) (2021).
- [31] M. Kupczynski, Is the moon there if nobody looks: Bell inequalities and physical reality, *Frontiers Phys.* [10.3389/fphy.2020.00273](#) (2020).
- [32] J. Foo, E. Asmodelle, A. P. Lund, and T. C. Ralph, Relativistic bohmian trajectories of photons via weak measurements, *Nature Commun.* **13**, [10.1038/s41467-022-31608-6](#) (2022).
- [33] A. Barchielli, L. Lanz, and G. Prosperi, A model for the macroscopic description and continual observations in quantum mechanics, *Nuovo Ciimento* **72B**, 79 (1982).
- [34] G. C. Ghirardi, A. Rimini, and T. Weber, Unified dynamics for microscopic and macroscopic systems, *Phys. Rev. D* **34**, 470 (1986).
- [35] G. C. Ghirardi, P. Pearle, and A. Rimini, Markov processes in hilbert space and continuous spontaneous localization of systems of identical particles, *Phys. Rev. A* **42**, 78 (1990).
- [36] S. H. Strogatz, From kuramoto to crawford: exploring the onset of synchronization in populations of coupled oscillators, *Physica D* **143**, 1 (2000).
- [37] S. H. Strogatz and I. Stewart, Coupled oscillators and biological synchronization, *Sci. Am.* **269**, 102 (1993).
- [38] J. Acebrón, L. Bonilla, C. Pérez-Vicente, F. Ritort, and R. Spigler, The kuramoto model: a simple paradigm for synchronization phenomena, *Rev. Mod. Phys.* **77**, 137 (2005).
- [39] J. D. daFonseca and C. V. Abud, The kuramoto model revisited, *J. Stat. Mech.* **2018**, 103204 (2018).
- [40] S.-Y. Ha, D. Ko, J. Park, and X. Zhang, Collective synchronization of classical and quantum oscillators, *EMS Surv. Math. Sci.* **3**, 209 (2016).
- [41] S. Gherardini, S. Gupta, and S. Ruffo, Spontaneous synchronisation and nonequilibrium

- statistical mechanics of coupled phase oscillators, *Contemp. Phys.* **59**, 229 (2018).
- [42] F. A. Rodrigues, T. K. D. Peron, P. Ji, and J. Kurths, The kuramoto model: in complex networks, *Phys. Rep.* **610**, 1 (2016).
 - [43] T. Vicsek and A. Zafeiris, Collective motion, *Phys. Rep.* **517**, 71 (2012).
 - [44] C. K. Hemelrijk and H. Hildenbrandt, Schools of fish and flocks of birds: their shape and internal structure by self-organization, *Interface Focus* **2**, 726 (2012).
 - [45] D. Bell-Pedersen, V. M. Cassone, D. J. Earnest, S. S. Golden, P. E. Hardin, T. L. Thomas, and M. Zoran, Circadian rhythms from multiple oscillators: Lessons from diverse organisms, *Nature Rev. Genetics* **6**, 544–556 (2005).
 - [46] L. Glass, Synchronization and rhythmic processes in physiology, *Nature* **410**, 277 (2001).
 - [47] M. Din, T. Danino, A. Prindle, M. Skalak, J. Selimkhanov, K. Allen, E. Julio, E. Atolia, L. Tsimring, S. N. Bhatia, and J. Hasty, Synchronized cycles of bacterial lysis for in vivo delivery, *Nature* **536**, 81 (2016).
 - [48] M. Diesmann, M.-O. Gewaltig, and A. Aertsen, Stable propagation of synchronous spiking in cortical neural networks, *Nature* **402**, 529 (1999).
 - [49] J. F. Hipp, A. K. Engel, and M. Siegel, Oscillatory synchronization in large-scale cortical networks predicts perception, *Neuron* **69**, 387–396 (2011).
 - [50] P. Fries, Rhythms for cognition: Communication through coherence, *Neuron* **88**, 220 (2015).
 - [51] M. Xu, D. Tieri, E. Fine, J. Thompson, and M. Holland, Synchronization of two ensembles of atoms, *Phys. Rev. Lett.* **113**, 154101 (2014).
 - [52] G. D. Scholes, Polaritons and excitons: Hamiltonian design for enhanced coherence, *Proc. R. Soc. A* **476**, 20200278 (2020).
 - [53] G. D. Scholes, The kuramoto-lohe model and collective absorption of a photon, *Proc. R. Soc. A* **478**, 20220377 (2022).
 - [54] M. A. Lohe, Non-abelian kuramoto models and synchronization, *J. Phys. A: Math. Theor.* **42**, 395101 (2009).
 - [55] M. A. Lohe, Quantum synchronization over quantum networks, *J. Phys. A: Math. Theor.* **43**, 465301 (2010).
 - [56] S.-H. Choi and S.-Y. Ha, Emergent behaviors of quantum lohe oscillators with all-to-all

- coupling, J. Nonlinear Sci. **25**, 1257 (2015).
- [57] R. W. Farebrother, J. Gross, and S.-O. Troschke, Matrix representation of quaternions, Linear Alg. Appl. **362**, 251 (2003).
 - [58] G. D. Scholes, A molecular perspective on quantum information, Proc. R. Soc. A **479**, 20230599 (2023).
 - [59] K. Kraus, *States, Effects, and Operations: Fundamental Notions of Quantum Theory*, Vol. 190 (Lecture Notes in Physics, Springer, Berlin, 1983).
 - [60] R. Bhatia, *Positive definite matrices* (Princeton University Press, Princeton, 2007).
 - [61] E. Størmer, *Positive Linear Maps of Operator Algebras* (Springer, Heidelberg, 2013).
 - [62] V. I. Paulsen, *Completely bounded maps and dilations* (Longman Scientific and Technical, New York, 1986).
 - [63] W. H. Zurek, Decoherence, einselection, and the quantum origins of the classical, Rev. Mod. Phys. **75**, 715 (2003).
 - [64] P. C. E. Stamp, Environmental decoherence versus intrinsic decoherence, Phil. Trans. R. Soc. A **370**, 4429 (2012).
 - [65] G. C. Ghiardi, A. Rimini, and T. Weber, The puzzling entanglement of schrödinger's wave function, Found. Phys. **18**, 1 (1988).
 - [66] H.-P. Breuer and F. Petruccione, *The Theory of Open Quantum Systems* (Oxford University Press, Oxford, 2007).